CHEMISTRY
A EUROPEAN JOURNAL

DOI: 10.1002/chem.201001424

Functionalized Alkynylplatinum(II) Polypyridyl Complexes for Use as Sensitizers in Dye-Sensitized Solar Cells

Eric Chi-Ho Kwok, Mei-Yee Chan, Keith Man-Chung Wong, Wai Han Lam, and Vivian Wing-Wah Yam*[a]

Abstract: A series of platinum(II) alkynyl-based sensitizers has been synthesized and found to show light-to-electricity conversion properties. These dyes were developed as sensitizers for the application in nanocrystalline TiO_2 dye-sensitized solar cells (DSSCs). Their photophysical and electrochemical properties were studied. The excited-state property was probed using nanosecond transient absorption spectroscopy, which showed the formation of a charge-separated state that arises from the intramolecular photoinduced charge transfer from the platinum(II) alkynylbithienylbenzothiadiazole moiety (donor) to the polypyridyl ligand (acceptor). A lifetime of 3.4 μs was observed for the charge-separated state. A dye-sensitized solar cell based on one of the complexes showed a short-circuit photocurrent of 7.12 mA cm^{-2}, an open circuit voltage of 780 mV, and a fill factor of 0.65, thus giving an overall power conversion efficiency of 3.6%.

Keywords: density functional calculations · dyes/pigments · energy conversion · platinum · sensitizers

Introduction

There has been fast-growing interest in the search for organic and polymeric materials for photovoltaic applications because they show promise in the fabrication of low-cost, flexible devices for renewable sources of energy.[1] Tremendous progress has also been made in the development of dye-sensitized solar cells (DSSCs) based on nanocrystalline TiO_2 semiconductors and well-designed panchromatic dye such as the black dye of formula $[Ru\mathbf{L}(NCS)_3]^-$, in which **L** is the anchoring 4,4′,4″-tricarboxy-2,2′:6′,2″-terpyridine ligand with reported efficiency of as high as 10.4%.[2]

The photochemistry of transition-metal complexes with polypyridine ligands has been extensively investigated in the last few decades.[3–6] With the advantages of possessing intense charge-transfer (CT) absorptions with large extinction coefficients, ease of tunability of redox properties, and good charge-transport properties, transition-metal complexes with polypyridyl ligands have attracted much attention for use in photovoltaic applications.[7–9] Grätzel and co-workers have demonstrated the photoelectrochemical properties of the heteroleptic amphiphilic complexes of formula $[Ru\mathbf{L}(NCS)_3]^-$ (**L** is the anchoring 4,4′,4″-tricarboxy-2,2′:6′,2″-terpyridine ligand).[2] With a high open-circuit voltage (V_{oc} = 0.72 V), a high short-circuit current (J_{sc} = 20.53 mA cm^{-2}), and a good fill factor value (FF = 0.74), this dye was shown to exhibit a relatively high conversion efficiency value of 10.4%.[2] A further remarkable increase in photovoltaic performance was achieved by Grätzel and co-workers using the complex with formula $[Ru\mathbf{L}\mathbf{L}'(NCS)_2]$, in which **L** is the anchoring 4,4′-dicarboxy-2,2′-bipyridine ligand and **L′** is 2,2′-bipyridine ligand with long alkyl chains.[8a,b] However, progress in optimizing dye-sensitized solar cells has been mainly focused on ruthenium-based sensitizers, partly due to the well-established photophysical and photochemical studies of the ruthenium(II) polypyridine system.[9a–d] Apart from the ruth-

[a] E. C.-H. Kwok, Dr. M.-Y. Chan, Dr. K. M.-C. Wong, Dr. W. H. Lam, Prof. Dr. V. W.-W. Yam
Institute of Molecular Functional Materials
Areas of Excellence Scheme
University Grants Committee (Hong Kong))
Department of Chemistry and
HKU-CAS Joint Laboratory of New Materials
The University of Hong Kong
Pokfulam Road, Hong Kong (P.R. China)
Fax: (+852) 2857-1586
E-mail: wwyam@hku.hk

Supporting information for this article is available on the WWW under http://dx.doi.org/10.1002/chem.201001424. It contains Cartesian coordinates for the optimized structures of **1** and **4**, spatial plots of selected molecular orbitals of **1** and **4**, and transient absorption difference spectra of **2** and **6** in CH_2Cl_2.

enium(II) system, studies on the isoelectronic osmium(II),[10a] rhenium(I),[10b] and iridium(III)[11c,d] polypyridines have also been reported. It was only in the last two decades or so that exploration of the photophysical properties of charge-transfer complexes have been extended to metal complexes other than the d^6-metal polypyridines, such as those of platinum(II)[12,13a] and copper(I).[11a,b]

Recent work on square-planar d^8 platinum(II) complexes showed that these complexes usually display an intense charge-transfer absorption band in the visible region that could readily be tuned by variation of the electronic properties of the terpyridyl and alkynyl ligands.[14a–d] We recently showed that with the incorporation of appropriate donor–acceptor ligands, their intense charge-transfer bands could be extended into the near-infrared (NIR) region.[14d] In view of this, together with the highly tunable nature of their photophysical and electrochemical properties, platinum(II) polypyridine complexes are envisaged to serve as a good candidate for the study of their photosensitizing behavior, which may play an important role in the development of new classes of molecular materials for dye-sensitized solar cell application studies. Recent works by Eisenberg,[13b–d] Sakai,[13e–g] Bernhard,[13h–j] and others have demonstrated the photosensitizing behavior of platinum(II) and iridium(III) polypyridyl complexes for the photogeneration of hydrogen. Sugihara[13k] recently reported the use of the dithiolatoplatinum(II) polypyridines for DSSC applications.

Electron transfer from the excited electronic state of the dye molecules adsorbed on the TiO_2 surface is a process of considerable practical importance in dye-sensitized solar cells. Various aspects of this process have been utilized and studied since the end of the last century and applied in the study of solar cells.[11e] Previous reports have shown that electron injection from Ru(tpy/bpy) into the TiO_2 conduction band proceeded at a rate from femtoseconds to picoseconds.[11f,g] Under such conditions, the nature of the excited state from which charge injection occurs is a metal-to-ligand charge-transfer process (MLCT), and similar rates of charge transfer from the excited state of the platinum(II) complexes into TiO_2 are expected. In general, a long-lived charge-separated state is preferable because electrons are able to migrate into the conduction band of TiO_2 in a more efficient way. Typically, studies of photoinduced charge separation and characterization of charge-separated (CS) states are probed by transient absorption measurements. Eisenberg and co-workers showed that some donor–acceptor platinum(II) complexes (D–Pt–A), in which Pt is linked to an electron donor (D) and acceptor (A), undergo photoinduced charge separation to produce the CS state D^+–Pt–A^- with lifetimes of 75–230 ns.[19b,f,g] These rather short decaying lifetimes have been attributed to the occurrence of rapid back electron transfer or charge recombination in the partial CS states (D^+–Pt^-–A or D–Pt^+–A^-). Schanze and co-workers have synthesized a series of platinum(II) alkynyl polymers that showed photoinduced electron transfer and a high quantum efficiency of charge separation. This process decayed with a lifetime of approximately 1–2 μs, with an enhanced solar-cell efficiency compared to the devices based on a wide-band-gap platinum(II) alkynyl polymer.[20a–c]

Herein, we provide a detailed report of the synthesis, photophysical and electrochemical characterization of a series of donor–acceptor platinum(II) polypyridyl alkynyl complexes and their sensitizing behavior for TiO_2-based dye-sensitized solar-cell applications. The nature of the excited state has also been probed using nanosecond transient absorption spectroscopy. Density functional theory (DFT) and time-dependent density functional theory (TDDFT) calculations have been performed to provide further insights into the nature of the excited states and the transitions in the electronic absorption study.

Results and Discussion

Synthesis and characterization: Platinum terpyridyl and bipyridyl alkynyl complexes **1**–**6** were synthesized by modification of a literature method for the synthesis of [Pt(tpy)Cl]$^+$ and [Pt(bpy)Cl_2].[14f–i] The [Pt(tpy)Cl]$^+$ or [Pt(bpy)Cl_2] precursor was dissolved in degassed dichloromethane or *N,N*-dimethylformamide that contained triethylamine, and the corresponding alkyne and a catalytic amount of copper(I) iodide were added. Metathesis reactions of complexes **1**–**4** with tetra-*n*-butylammonium hydroxide in aqueous solution gave the respective complexes as the tetra-*n*-butylammonium salt. Complexes **1**–**6** have been characterized by ^{1}H NMR spectroscopy and IR, FAB, and ESI mass spectrometry and gave satisfactory elemental analyses.

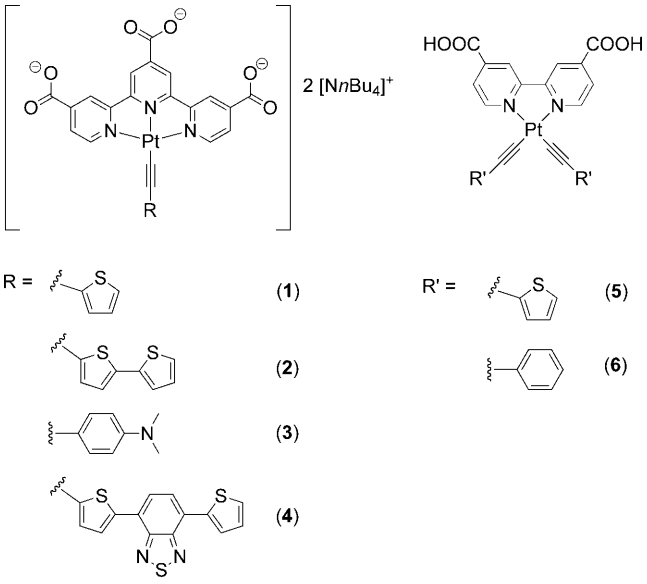

Electronic absorption and emission studies: The electronic absorption spectra of complexes **1**–**6** exhibit an intense absorption band at 302–388 nm and a less intense absorption band at 412–534 nm in methanol and *N,N*-dimethylformamide at 298 K (Figure 1a). The electronic absorption data

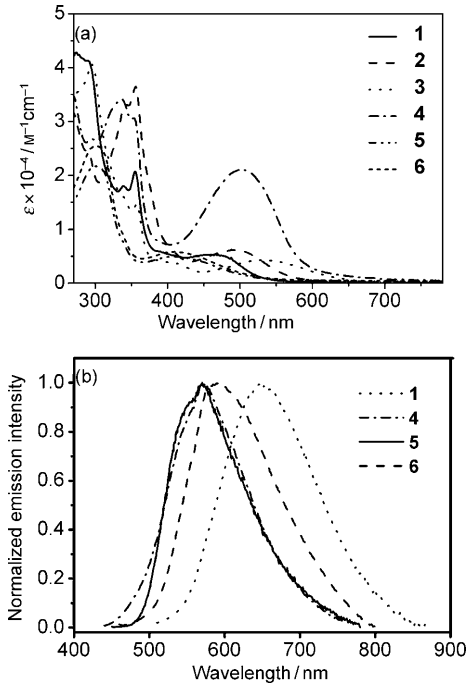

Figure 1. a) Electronic absorption spectra of complexes **1**–**4** in MeOH and complexes **5** and **6** in DMF. b) Emission spectra of complexes **1** and **4** in MeOH and **5** and **6** in DMF.

are summarized in Table 1. With reference to the previous studies on the related system of $[Pt(N^N^N)(C\equiv C-R)]^+$ and $[Pt(N^N)(C\equiv C-R)_2]$ complexes (N^N^N = terpyridyl ligand; N^N = bipyridyl ligand),[14a–e,16,17] the high-energy absorptions located at about 302–388 nm are assigned as the intraligand (IL) $\pi\rightarrow\pi^*$(C≡C–R) and $\pi\rightarrow\pi^*$(tctpy/dcbpy) transitions of the respective alkynyl and substituted polypyridine ligands (tctpy = 4,4′,4″-tricarboxy-2,2′:6′,2″-terpyridine; dcbpy = 4,4′-dicarboxy-2,2′-bipyridine), whereas the low-energy band located in the visible region is assigned to an admixture of metal-to-ligand charge transfer (MLCT) [$d\pi$(Pt)→π^*(tctpy/dcbpy)] and alkynyl-to-polypyridine ligand-to-ligand charge transfer (LLCT) [π(C≡C–R)→π^*(tctpy/dcbpy)] transitions. Interestingly, for complexes that contain strongly electron-donating groups on the alkynyl ligands, a substantial mixing of LLCT character has been observed (vide infra). For complex **4**, closer scrutiny of the absorption spectrum showed that the band in this region has a molar extinction coefficient on the order of 10^4 dm^{3}mol^{-1}cm^{-1}, which is much larger than the order of 10^3 dm^{3}mol^{-1}cm^{-1} commonly observed for platinum(II) polypyridyl MLCT/LLCT transitions.[14a–e] Further examination of the free ligand associated with complex **4**—that is, the Th–BTD–Th ligand—showed that it absorbed strongly in the same region with molar extinction coefficients on the order of 10^4 dm^{3}mol^{-1}cm^{-1}. Therefore it is likely that the lowest-energy absorption band in complex **4** would consist

Table 1. Photophysical and electrochemical data of complexes **1**–**6**.

Complex	λ_{max}[a] [nm] (ε_{max} [M^{-1}cm^{-1}])	Medium (T [K])	Emission λ_{em} [nm] (τ_o [μs])	Emission ϕ_{em}[b]	Oxidation E_{pa} [V][c,d] vs. SCE	Reduction $E_{1/2}$ [V][c,d] vs. SCE	$E_{0\text{-}0}$ [eV]	E [$Pt^{3+/2+*}$] [V] vs. SCE
1	336 (18260), 356 (20680), 400 (5480), 460 (5690)	MeOH (298)	650 (0.64)	5.2×10^{-4}	+0.91	−1.09	2.24	−1.33
		solid (298)	–[e]			−1.58		
		solid (77)	–[e]					
		glass[f] (77)	–[e]					
2	356 (36490), 406 (6265), 492 (6170)	MeOH (298)	–[e]	–	+0.75	−1.07	–	–
		solid (298)	–[e]			−1.55		
		solid (77)	–[e]					
		glass[f] (77)	–[e]					
3	290 (40550), 340 (16000), 356 (14600), 534 (4300)	MeOH (298)	–[e]	–	+0.62	−1.09	–	–
		solid (298)	–[e]			−1.60		
		solid (77)	–[e]					
		glass[f] (77)	–[e]					
4	304 (27000), 334 (34000), 352 (31000), 502 (21000)	MeOH (298)	570	1.2×10^{-6}	+0.50	−1.09	2.26	−1.76
		solid (298)	–[e]			−1.41		
		solid (77)	–[e]			−1.58		
		glass[f] (77)	–[e]					
5	302 (25430), 412 (5800)	DMF (298)	570 (0.85)	8.6×10^{-4}	+0.85	−0.83	2.80	−1.95
		solid (298)	566			−1.12		
		solid (77)	550					
		glass[f] (77)	620					
6	330 (25450), 414 (5790)	DMF (298)	592 (0.83)	8.4×10^{-4}	+0.86	−0.85	2.46	−1.60
		solid (298)	–[e]			−1.15		
		solid (77)	–[e]					
		glass[f] (77)	615					

[a] Electronic absorption data of complexes **1**–**4** were measured in MeOH; **5** and **6** were measured in DMF. [b] The luminescence quantum yield measured at room temperature using $[Ru(bpy)_3]Cl_2$ as a standard. [c] 0.1 M nBu$_4$NPF$_6$ (TBAH) in DMF as supporting electrolyte at room temperature; scan rate, 100 mV s^{-1}. [d] E_{pa} refers to the anodic peak potential for the irreversible oxidation waves. $E_{1/2} = (E_{pa} + E_{pc})/2$; E_{pa} and E_{pc} are peak anodic and peak cathodic potentials, respectively. [e] Nonemissive. [f] In butyronitrile glass.

of an admixture of IL $\pi\rightarrow\pi^*$(C≡C−R) and MLCT/LLCT transitions.

Upon photoexcitation, complexes **1**, **5**, and **6** displayed intense emission bands at around 570–650 nm in fluid solution at 298 K. Complex **4** showed a weakly emissive band at approximately 570 nm, whereas complexes **2** and **3** were nonemissive. In frozen ethanol/methanol (4:1 v/v) glass at 77 K, complexes **5** and **6** displayed emission bands at higher energies, with vibrational progressional spacings of around 1300 cm^{-1}, which is typical of the skeletal vibrational modes of the bipyridine ligand. With reference to the previous spectroscopic studies on the related complexes [Pt(N^N^N)(C≡C−R)]$^+$ and [Pt(N^N)(C≡C−R)$_2$] complexes,[14a–c,16] an emission origin of an ^{3}MLCT [dπ(Pt)→π*(tctpy/dcbpy)]/^{3}LLCT [π(C≡C−R)→π*(tctpy/dcbpy)] excited state is tentatively assigned to complexes **1**, **5**, and **6**, whereas the weakly emissive band of complex **4** is tentatively assigned to have originated from a metal-perturbed intraligand (IL) state. The photophysical data are tabulated in Table 1. In addition, the emission behavior of complex **5** was chosen for study on both TiO_2 film and on quartz substrate, since only complex **5** emits in the solid state. No emission was observed. The nonemissive nature on TiO_2 film of complex **5** may be attributed to the quenching by the electron injection from the excited state of the complexes to the conduction band of the TiO_2 nanoparticles.

Electrochemical study: Since the energy levels of the frontier orbitals of the sensitizers play an important role in the electron-transfer processes in dye-sensitized solar cells, the electrochemical behaviors of **1**–**6** have been studied. The energy levels of the HOMOs and LUMOs were derived from the oxidation potentials and reduction potentials. In general, the cyclic voltammograms of complexes **1**–**3** displayed two quasireversible reduction couples at −1.07 to −1.60 V (versus the saturated calomel electrode (SCE)) and an irreversible anodic wave at approximately +0.62 to +0.91 V (versus SCE), whereas complex **4** displayed three quasireversible reduction couples at −1.09 to −1.58 V (versus SCE) and an irreversible anodic wave at around + 0.50 V (versus SCE). Complexes **5** and **6** displayed two quasireversible reduction couples at around −0.83 to −1.15 V and an irreversible anodic wave at around +0.85 to +0.86 V (versus SCE). The two quasireversible reduction couples in complexes **1**–**3**, **5**, and **6**, which are independent of the nature of the substituents on the alkynyl ligand, are assigned as the two successive reductions of the polypyridine ligand.[14b,e,15a–b,16c,17a] Similarly, the reduction couples of complex **4** at around −1.09 and −1.58 V are assigned as the reductions of the terpyridine ligand, whereas the additional quasireversible reduction couple at approximately −1.41 V (versus SCE) is assigned as the reduction of the bithienylbenzothiadiazole alkynyl ligand. The electrochemical data for complexes **1**–**6** are summarized in Table 1, and the cyclic voltammograms are shown in Figure 2.

In general, the oxidation wave was found to occur at more positive potential for the compounds with less π-donating or less electron-rich alkynyl ligands attached to the metal center, that is, **1** (+0.91 V) > **2** (+0.75 V) > **3** (+0.62 V) > **4** (+0.50 V) for the terpyridyl analogues, which is in line with the electron richness of the substituent on the alkynyl ligand; whereas complexes **5** and **6** showed similar anodic potentials, thus resulting in the energy of the dπ(Pt)/pπ(C≡C−R) orbital in the order of **1** < **2** < **3** < **4** for the terpyridyl analogues and **5**≅**6** for the bipyridyl analogues. With reference to previous electrochemical studies of the related compounds, this irreversible oxidation wave is ascribed to the mixed platinum(II)/alkynyl-centered oxidation process. Similar trends have also been reported in other related alkynylplatinum(II) polypyridyl complexes.[14b,e,15a,b,16c]

Computational studies: To gain further insight into the nature of the excited states and the transitions in the high-energy and low-energy absorption bands of the platinum(II) polypyridyl alkynyl complexes, complexes **1** and **4** were chosen for the computational study (for details, see the Experimental Section). Geometry optimization of complexes **1**

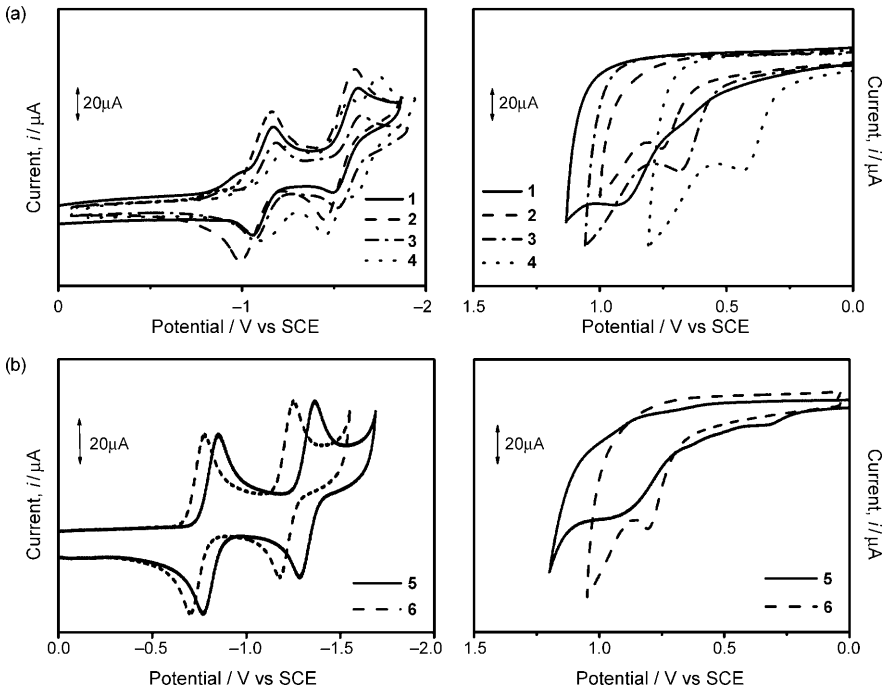

Figure 2. Cyclic voltammograms of complexes a) **1**–**4** and b) **5** and **6**.

and **4** starts from a structure in which the plane of the thienyl and dithienylbenzothiadiazole rings are coplanar with the plane of the Pt terpyridyl unit, respectively. The optimized structures and selected structural parameters are shown in Figure 3. The average Pt–N, Pt–C(alkynyl) and C≡C bond distances in **1** are found to be 2.009, 1.958, and 1.231 Å, respectively, which are very close to those found in complex **4**.

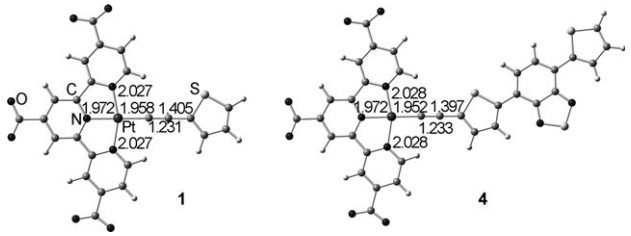

Figure 3. The optimized geometries for **1** and **4** with selected structural parameters.

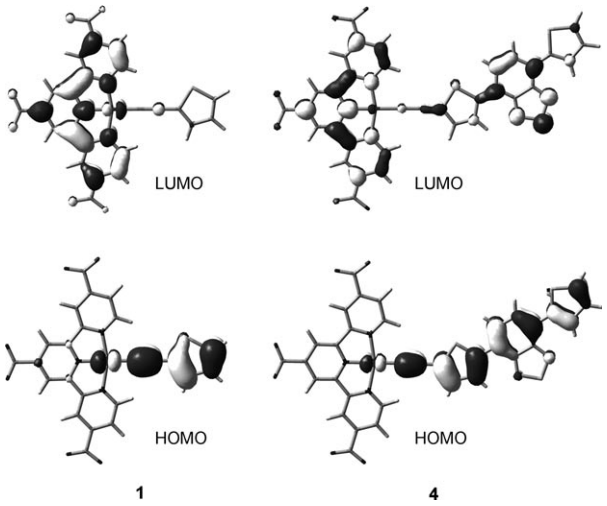

Figure 4. Spatial plots (isovalue = 0.03) of the HOMO and LUMO of **1** and **4** obtained from TDDFT/CPCM (CH_3OH) calculation.

A nonequilibrium TDDFT/CPCM calculation using CH_3OH as the solvent was employed to compute the first twenty-five singlet–singlet transitions of complexes **1** and **4**. Selected singlet–singlet transitions with oscillator strength (f) > 0.2 are listed in Table 2. The spatial plots of the molecular orbitals involved in the transitions are shown in Figure S1 in the Supporting Information, with the exception of the HOMO and LUMO, which are shown in Figure 4. The first singlet–singlet transition of **1** and **4** with significant oscillator strengths correspond to the excitation from the HOMO to the LUMO. As shown in Figure 4, the HOMO for **1** and **4** are the out-of-plane highest-occupied π orbitals of the respective C≡C–C_4H_3S and C≡C–$C_{14}H_7N_2S_3$ units, mixed with metal dπ orbitals of proper symmetry in an antibonding fashion. The LUMO for **1** is essentially the π* orbitals localized on the tricarboxyterpyridyl ligand, whereas the LUMO for **4** is the π* orbital of the tricarboxyterpyridyl ligand with some mixing of the π* orbital of the C≡C–$C_{14}H_7N_2S_3$ unit. Based on the TDDFT/CPCM calculations, the low-energy absorption band can be assigned to an admixture of MLCT [dπ(Pt)→π*(tctpy)] and LLCT [π(C≡C–R)→π*(tctpy)] transition for **1**, whereas for **4** the MLCT [dπ(Pt)→π*(tctpy)]/LLCT [π(C≡C–R)→π*(tctpy)] transition is mixed with IL π→π* transitions of the C≡C–$C_{14}H_7N_2S_3$ ligand. The larger oscillator strength computed for the $S_0 \rightarrow S_1$ transition in **4** relative to **1** is in line with the larger extinction coefficient observed for the low-energy absorption band in **4**, which further supports the low-energy absorption band in **4** as consisting of the mixing of an IL (C≡C–$C_{14}H_7N_2S_3$) character.

Several transitions are computed in the region of the intense high-energy absorption band of **1** and **4**. Table 2 lists the two most intense transitions. For **1**, the most intense transition ($S_0 \rightarrow S_{14}$) computed at 323 nm involves the excitation from the π orbital of the tctpy ligand mixed with metal dπ orbital to the LUMO, and it can be assigned as the IL π→π* transition of the tctpy ligand mixed with some MLCT [dπ(Pt)→π*(tctpy)] character. A similar type of IL/MLCT [π(tctpy)/dπ(Pt)→π*(tctpy)] transition ($S_0 \rightarrow S_{21}$) can be also found in **4**, which is computed at 322 nm. In addition to this transition, a transition ($S_0 \rightarrow S_9$) computed at 360 nm that is derived from the HOMO→LUMO+3 and HOMO→LUMO+5 excitations is found to be very intense. The LUMO+3 and LUMO+5 are the π* orbitals localized on

Table 2. Selected singlet-excited states (S_n) of **1** and **4** computed by TDDFT/CPCM (CH_3OH) calculations, with the orbitals involved in the excitations (H = HOMO and L = LUMO), transition coefficients, vertical excitation wavelengths [nm], oscillator strengths (f), and character of the excited state.

Complex	S_n	Excitation[a]	λ [nm]	f[b]	Character
1	S_1	H→L (0.69)	508	0.222	MLCT/LLCT [dπ(Pt)/π(C≡C–R)→π*(tctpy)]
	S_{14}	H−11→+L (0.63)	323	0.421	IL/MLCT [π(tctby)/dπ(Pt)→π*(tctpy)]
	S_{20}	H−12→L (0.36)	300	0.396	ILCT [p(O)→π*(tctpy)][c]
		H−2→L+1 (0.37)			IL/MLCT [π(tctpy)/dp(Pt)→π*(tctpy)]
		H→L+4 (−0.35)			MLCT/IL [dπ(Pt)/π(C≡C–R)→π*(C≡C–R)]
4	S_1	H→L (0.66)	600	0.929	MLCT/LLCT/IL [dπ(Pt)/π(C≡C–R)→π*(tctpy)/π*(C≡C–R)]
	S_9	H→L+3 (0.51)	360	0.713	MLCT/LLCT [dπ(Pt)/π(C≡C–R)→π*(tctpy)]
		H→L+5 (0.44)			MLCT/IL [dπ(Pt)/π(C≡C–R)→p*(C≡C–R)]
	S_{21}	H−13→L (0.46)	322	0.339	IL/MLCT [π(tctpy)/dπ(Pt)→π*(tctpy)/π*(C≡C–R)]
		H−1→L+2 (−0.36)			LLCT/MLCT [π(C≡C–R)/dp(Pt)→π*(tctpy)]

[a] The excitations with transition coefficients less than the absolute value of 0.3 were not shown. [b] Only the transitions with oscillator strength greater than 0.2 are listed. [c] Transition involves the excitation from out-of-plane p orbitals of carboxyl oxygen atoms to the π* orbital of the dcbpy ligand.

the tricarboxyterpyridyl and C≡C−$C_{14}H_7N_2S_3$ ligands, respectively. Therefore, the transition can be assigned to an admixture of the LLCT [π(C≡C−R)→π*(tctpy)] and IL π→π* of the C≡C−R ligand transitions.

Nanosecond UV/Vis transient absorption (TA) spectroscopy: To probe the nature of the excited states, nanosecond TA measurements were performed on complexes **1**–**6** at room temperature in degassed CH_2Cl_2. The nanosecond TA spectra for complexes **1**, **4**, and **5** are shown in Figure 5. The transient absorption spectra of **2** and **6** are shown in Figure S2 in the Supporting Information. All the spectra were collected immediately after excitation at 355 nm and the transient absorption spectra of complexes **1**–**3** and **5**–**6** are virtually identical to those previously reported for other related platinum(II) polypyridyl complexes.[19]

Upon laser excitation, the platinum(II) terpyridyl and bipyridyl alkynyl complexes undergo electron-density redistribution toward the terpyridine or bipyridine moieties. For complexes **1**–**3**, the TA spectra showed two positive absorption bands at around 380 and 500–550 nm and a broad absorption band that extends into the NIR region (690–800 nm) and continues beyond our detection range; these are commonly assigned to the terpyridine radical anion absorption that results from the ^{3}MLCT [dπ(Pt)→π*(tctpy)]/^{3}LLCT [π(C≡CR)→π*(tctpy)] excited state.[19] Bleaching was found in the spectrum of complex **2** at approximately 440–480 nm, ascribed to the depletion of the ground state MLCT/LLCT absorption, whereas no ground-state bleaching was found in complexes **1** and **3**. The transient absorption bands of complexes **1**–**3** decay through first-order kinetics to their respective ground state with no difference in the transient decay profile at different wavelengths. The transient absorption decay profiles for complexes **1**–**3** were about 1–2 μs, which is consistent with the emission-decay lifetimes of the respective complexes and are assigned to the ^{3}MLCT/^{3}LLCT excited-state absorption. Similarly, complexes **5** and **6** showed absorption bands at approximately 360 and 480 nm and a broad absorption band that extends into the NIR region (690–800 nm). The TA spectral features are characteristic of the absorption of the bipyridine radical anion that results from the ^{3}MLCT/^{3}LLCT state. The negative signal centered at around the emission maximum of complex **6** (580–630 nm) was ascribed to the ^{3}MLCT/^{3}LLCT emission.

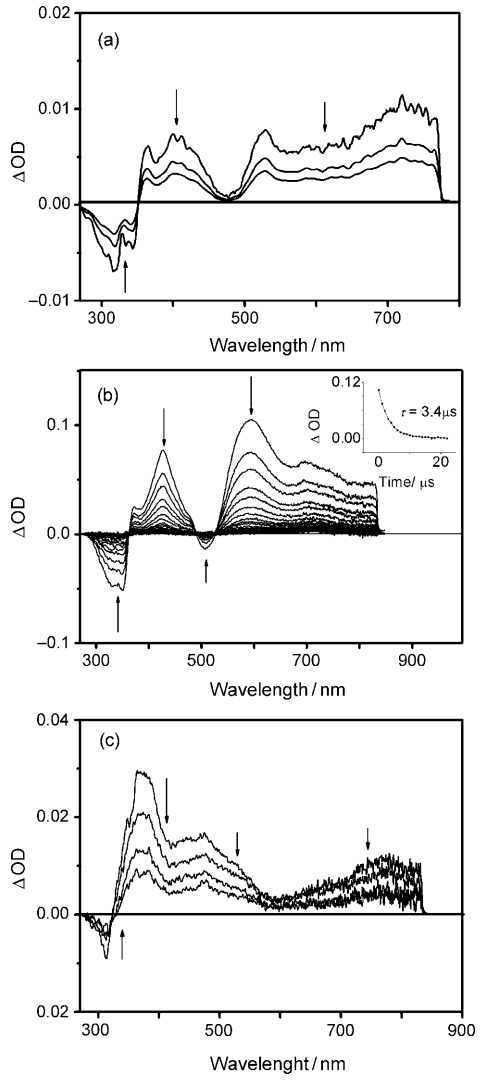

Figure 5. Transient absorption difference spectra of a) **1**, b) **4**, and c) **5** measured in CH_2Cl_2 following a 355 nm laser pulse.

Although complexes **1**–**3**, **5**, and **6** all showed transient absorption signals typical of the ^{3}MLCT/^{3}LLCT absorption with decay profiles in agreement with those of the emissive-state lifetimes, the transient absorption spectrum of complex **4** showed very long-lived strong absorption bands at around 360–480 nm and 530–670 nm and a very broad band that extends into the NIR region (690–800 nm). Similar to complexes **1**–**3**, the positive absorption bands are characteristic of the terpyridine radical anion. Ground-state bleaching was found in the spectrum of complex **4** at around 490–530 nm, again ascribed to the ground-state MLCT/LLCT absorption. Well-defined isosbestic points were observed at approximately 360, 480, and 530 nm. The transient signals were found to show a monoexponential decay of 3.4 μs, which is on a much longer timescale than that of the emission lifetime. It is believed that the absorption at around 580 nm is attributed to the formation of the bithienylbenzothiadiazole radical cation. Therefore, the long-lived transient signal is tentatively assigned to result from the formation of a charge-separated state, which can be alternatively described as a [Pt(tctpy)$^{-\bullet}$−(C≡C-Th-BTD-Th)$^{+\bullet}$] state, with the charge recombination rate constant determined to be $2.9\times10^5\ s^{-1}$.

Photocurrent–voltage characteristics of Pt-dye-coated TiO_2 electrode: The current–voltage curves of the cells based on these new sensitizers obtained both in the dark and under illumination of air mass (AM) 1.5 G sunlight (100 mW cm^{-2}) are shown in Figure 6a with the dye-sensitized TiO_2 electrode systems in this study. The short-circuit current (J_{sc}) and open-circuit voltage (V_{oc}) values for each dye-sensitized

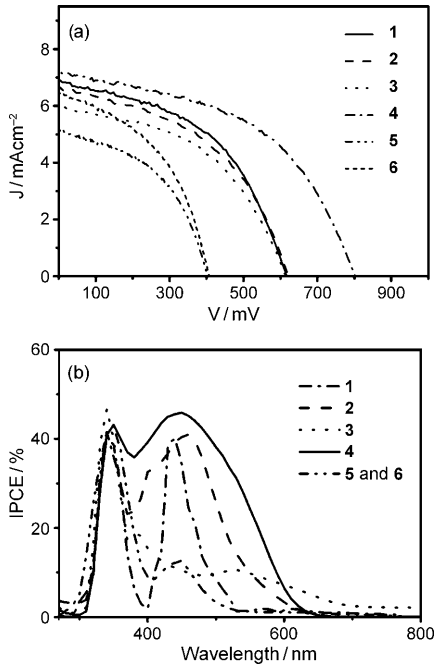

Figure 6. a) *I–V* characteristics of the devices fabricated from **1–6** measured under AM 1.5 G illumination. b) Photocurrent action spectra of nanocrystalline TiO_2 films sensitized by complexes **1–6**.

TiO_2 electrode with an electrolyte that contained 0.6 M 1,3-dimethylimidazolium iodide (DMII), 0.05 M I_2, 0.5 M *tert*-butylpyridine (TBP), and 0.1 M LiI in methoxyacetonitrile were recorded. An estimation of the excited-state reduction potential using the spectroscopic E_{0-0} value of 2.24 eV for **1**, 2.26 eV for **4**, 2.80 eV for **5**, and 2.46 eV for **6**, and electrochemical data E^0 of +0.91 V for **1**, +0.50 V for **4**, +0.85 V for **5**, and +0.86 V versus SCE for **6** would give the excited-state reduction potentials of −1.33, −1.76, −1.95, and −1.60 V versus SCE for complexes **1**, **4**, **5**, and **6**, respectively, which are sufficient to inject an electron into the conduction band of TiO_2 (−0.7 V vs. SCE).[13a,l] By assuming similar molecular-orbital geometry for all the complexes when anchored onto TiO_2, those complexes with the energy of the LUMO close to that of the anchoring group would enhance the orbital overlap with the titanium 3d orbital that favors electron injection from the dye to TiO_2. Table 3 summarizes the fill factor (*FF*) and the power-conversion efficiency (PCE) for complexes **1–6**, with the most efficient sensitizer [Pt(tctpy)(C≡C−$C_{14}H_7N_2S_3$)][N*n*Bu_4]$_2$ (**4**) exhibiting a photocurrent of 7.12 mA cm^{-2} and an open-circuit potential of 780 mV with a fill factor of 0.65 under the illumination of AM 1.5 G sunlight (100 mW cm^{-2}).

Table 3. The performance of dye-sensitized solar cells **1–6**.

Complex	J_{sc} [mA cm^{-2}]	V_{oc} [mV]	*FF*	PCE [%]	IPCE [%]
1	6.75	620	0.61	2.6	42 (340 nm); 40 (440 nm)
2	6.85	620	0.62	2.7	45 (340 nm); 40 (460 nm)
3	6.04	620	0.60	2.4	46 (340 nm); 10 (550 nm)
4	7.12	780	0.65	3.6	44 (340 nm); 46 (450 nm)
5	5.20	400	0.58	1.6	43 (340 nm); 13 (420 nm)
6	6.65	400	0.58	1.8	43 (340 nm); 13 (420 nm)

In general, the device performances of **1–4** are found to be higher than that of **5** and **6**, and the photocurrent density was found to increase with the extension of the π-conjugated system and the increase in electron-donating ability of the alkynyl donor functionality. On going from −C≡C−$C_6H_4NMe_2$ to −C≡C−$C_8H_5S_2$, an increase of the photocurrent density from 6.04 to 6.85 mA cm^{-2} was observed, in line with an increase in the π-conjugation. Upon further extension of the π-conjugation and an increase in the electron-donating ability to −C≡C−$C_{14}H_7N_2S_3$, the photocurrent density was further increased to 7.12 mA cm^{-2}. In addition, the high J_{sc} value for the device with **4** as the photosensitizer may also result from the relatively higher HOMO level of **4** than the other complexes, which may lead to a more facile regeneration of the oxidized dye. Figure 6b shows the photocurrent action spectra for [Pt(tctpy)(C≡C−R)]$^{2-}$ and [Pt(N^N)(C≡C−R′)$_2$] complexes adsorbed on TiO_2 films, with the incident photon-to-current conversion efficiency (IPCE) values plotted as a function of wavelength. The photocurrent action spectra of each dye-coated TiO_2 electrode collected under short-circuit conditions showed a strong correlation with the electronic absorption spectra of the metal complexes. The IPCE values of all complexes in this study are given in Table 3; **1**, **2**, and **4** show IPCE values of over 40% in the visible region. The $IPCE_{max}$ value follows the trend: **4** > **2** > **1** ≅ **3** > **5** ≅ **6**, with complexes **5** and **6** showing very low photosensitization properties. The low photocurrents are mainly due to the narrow absorption bands in the visible region, thus resulting in poorer light-harvesting ability under irradiation. The IPCE values increase in the order **4** > **2** > **1**, with complex **4** showing the highest IPCE coverage in the visible region. The same trend was also observed in the J_{sc} values (7.12, 6.85, and 6.75 mA cm^{-2} for complexes **4**, **2**, and **1**, respectively) and power-conversion efficiencies. The improved efficiency of complex **4** may attributed to the introduction of the strongly electron-donating bithienylbenzothiadiazole alkynyl substituent, which leads to the enhancement and redshifting of the MLCT/LLCT absorption band in the visible region and a long-lived charge-separated state as mentioned in the TA study. The improved light-harvesting efficiency and the resulting photocurrent generation are responsible for the remarkable difference in the PCE and IPCE values of complex **4**. However, the cell efficiencies of complexes **1–6** (1.6–3.6%) are relatively lower, compared to that of [Ru(dcbpy)$_2$(NCS)$_2$] dye (10.4%), which is probably due to the high ratios of the rates of recombination and self-quenching phenomenon that counteract the light-harvesting behavior of the dye. Similar findings were also observed and reported in other diiminepplatinum(II) and dithiolatoplatinum(II) polypyridine complexes by Eisenberg and Sugihara and co-workers.[9b,15c,18]

Conclusion

In summary, a number of square-planar alkynylplatinum(II) terpyridyl and bipyridyl complexes have been successfully synthesized that can sensitize TiO_2 for dye-sensitized solar-cell application studies. Their electrochemical, photophysical, luminescence, and photovoltaic properties have been studied. In the UV/Vis absorption study, complexes **1**–**6** show an intense charge-transfer absorption band in the visible region, and the majority of the complexes are found to exhibit stable solar-cell properties and convert light into electricity. The transient absorption study demonstrated that complexes **1**–**6** show spectral features typical of the terpyridine and bipyridine radical anion, with the signals of complexes **1**–**3** and **5** and **6** assigned as the absorption of the ^{3}MLCT/^{3}LLCT excited state. On the contrary, the transient absorption spectrum of complex **4** shows a long-lived transient signal that has been tentatively assigned to the absorption of the charge-separated [Pt(tctpy)$^{-\bullet}$–(C≡C-Th-BTD-Th)$^{+\bullet}$] state. Among the platinum complexes, a short-circuit current of 7.12 mA cm^{-2} and an open-circuit potential of 780 mV, with a fill factor of 0.65 and a power-conversion efficiency of 3.6% were obtained for the most efficient sensitizer [Pt(tctpy)(C≡C–$C_{14}H_7N_2S_3$)][N*n*Bu$_4$]$_2$ (**4**) under AM 1.5 G simulated solar irradiation. Further optimization of the molecular design and electrolyte combination such as introducing different donor–acceptor ligands with charge-transfer properties are promising strategies for achieving highly efficient platinum dye-sensitized solar-cells.

Experimental Section

Materials: All chemicals used for synthesis were of reagent grade and purchased from Sigma-Aldrich Chemical Co. and Strem Chemicals, Inc. 4,4′-Dicarboxylic acid-2,2′-bipyridine[28] and [Pt(dcbpy)Cl$_2$][28] were synthesized as described previously. 2,2′-Bithiophene, thiophen-2-ylboronic acid,[29] 4-ethynyl-*N*,*N*-dimethylbenzenamine,[14e] 4,4′-dicarboxylic acid-2,2′-bipyridine,[28] and 4-(5-bromothiophen-2-yl)-7-(thiophen-2-yl)-benzo[*c*][1,2,5]thiadiazole[30] were prepared as reported previously.

4,4′,4″-Triethyl-2,2′:6′,2″-terpyridine (Et$_3$tpy): This was synthesized according to a modification of the literature procedure reported by Grätzel and co-workers[1] by using freshly distilled 4-ethylpyridine and 10% Pd on activated carbon as starting materials.

4,4′,4″-Tricarboxy-2,2′:6′,2″-terpyridine (H$_3$tctpy): Et$_3$tpy (1.5 g) was added to a stirred solution of sulfuric acid (98%, 30 mL). Potassium dichromate (9.0 g) was added in small portions at a temperature below 70 °C. The mixture was poured into ice water (500 mL) and cooled overnight. The resulting solid was filtered and washed with water until the washings were colorless to yield a pale yellow solid (1.0 g). The resulting solid was heated to reflux in of 50% nitric acid (60 mL) for 6 h. The solution was poured into ice water (200 mL) and was allowed to be kept in the refrigerator overnight. The obtained precipitate was filtered and washed with water and Et$_2$O several times to give pure 4,4′,4″-tricarboxy-2,2′:6′,2″-terpyridine. Yield: 0.5 g (37%); ^{1}H NMR (400 MHz, D$_2$O/NaOD, 298 K, relative to Me$_4$Si): δ = 7.53 (d, J = 6.0 Hz, 2H; H5 and H5″), 8.43 (d, J = 6.0 Hz, 2H; H6 and H6″), 8.31 ppm (s, 2H; H3 and H3″).

[Pt(tctpy)Cl]OTf: The complex was prepared according to a modification of a method previously reported for the synthesis of chloroplatinum(II) terpyridyl complexes. Yield: 300 mg (78%); ^{1}H NMR (400 MHz, CD_3SOCD_3, 298 K, relative to Me$_4$Si): δ = 7.67 (d, J = 6.0 Hz, 2H; terpyridyl H), 8.38 (s, 2H; terpyridyl H), 8.41 (s, 2H; terpyridyl H), 8.99 (d, J = 6.0 Hz, 2H; terpyridyl H); MS (FAB$^+$): m/z: 744.0 $[M]^+$; elemental analysis calcd (%) for $C_{19}H_{11}ClF_3N_3O_9PtS$: C 30.64, H 1.50, N 5.64; found: C 31.02, H 1.74 N, 5.37.

Trimethyl(thiophen-2-ylethynyl)silane: A mixture of bis(triphenylphosphine)palladium(II) chloride (70 mg, 0.1 mmol) and copper(I) iodide (22 mg, 0.2 mmol) in distilled triethylamine (20 mL) was deaerated with nitrogen. 2-Bromothiophene and (trimethylsilyl)acetylene (0.6 g, 6 mmol) were then added to the reaction mixture and was stirred while being heated at reflux for 12 h. The mixture was then filtered, and the filtrate was evaporated to dryness under reduced pressure to give a solid residue. The residue was then dissolved in chloroform and purified by column chromatography on silica gel by using petroleum ether and dichloromethane as eluent. Yield: 1 g (86%); ^{1}H NMR (400 MHz, CD_3Cl_3, 298 K, relative to Me$_4$Si): δ = 0.29 (s, 9H; SiMe$_3$), 7.12 (d, J = 3.0 Hz, 1H; C_4H_3S), 7.18 (d, J = 3.0 Hz, 1H; C_4H_3S), 7.22 ppm (t, J = 3.0 Hz, 1H; C_4H_3S); MS (FAB$^+$): m/z: 180.0 $[M]^+$.

(2,2′-Bithiophen-5-ylethynyl)trimethylsilane: A mixture of 5-bromo-2,2′-bithiophene (1 g, 4.1 mmol), bis(triphenylphosphine)palladium(II) chloride (70 mg, 0.1 mmol), copper(I) iodide (22 mg, 0.2 mmol), and distilled triethylamine (20 mL) was deaerated with nitrogen. (Trimethylsilyl)acetylene (0.6 g, 6 mmol) was then added to the reaction mixture and was stirred while being heated at reflux for 12 h. The mixture was then filtered, and the filtrate was evaporated to dryness under reduced pressure to give a solid residue. The residue was then dissolved in chloroform and purified by column chromatography on silica gel by using petroleum ether and dichloromethane as eluent. Yield: 0.77 g (72%); ^{1}H NMR (400 MHz, $CDCl_3$, 298 K, relative to Me$_4$Si): δ = 0.26 (s, 9H; SiMe$_3$), 7.01 (m, J = 3.0 Hz, 2H; $C_8H_5S_2$), 7.13 (d, J = 3.0 Hz, 1H; $C_8H_5S_2$), 7.17 (d, J = 3.0 Hz, 1H; $C_8H_5S_2$), 7.23 ppm (t, J = 3.0 Hz, 1H; $C_8H_5S_2$); MS (FAB$^+$): m/z: 262.0 $[M]^+$.

4-(Thiophen-2-yl)-7-{5-[(trimethylsilyl)ethynyl]thiophen-2-yl}benzo[*c*]-[1,2,5]thiadiazole: A mixture of 4-(5-bromothiophen-2-yl)-7-(thiophen-2-yl)benzo[*c*][1,2,5]thiadiazole (1 g, 2.7 mmol), bis(triphenylphosphine)palladium(II) chloride (80 mg, 0.1 mmol), copper(I) iodide (22 mg, 0.2 mmol), and distilled triethylamine (20 mL) was deaerated with nitrogen. (Trimethylsilyl)acetylene (0.6 g, 6 mmol) was then added to the reaction mixture and was stirred while being heated at reflux for 12 h. The mixture was then filtered, and the filtrate was evaporated to dryness under reduced pressure to give a solid residue. The residue was then dissolved in chloroform and purified by column chromatography on silica gel by using petroleum ether and dichloromethane as eluent. Yield: 0.70 g (65%); ^{1}H NMR (400 MHz, $CDCl_3$, 298 K, relative to Me$_4$Si): δ = 0.26 (s, 9H; SiMe$_3$), 7.21 (t, J = 4.0 Hz, 1H; $C_{14}H_8N_2S_3$), 7.35 (d, J = 4.0 Hz, 1H; $C_{14}H_8N_2S_3$), 7.46 (d, J = 4.0 Hz, 1H; $C_{14}H_8N_2S_3$), 7.85 (d, J = 4.0 Hz, 1H; $C_{14}H_8N_2S_3$), 7.95 (d, J = 4.0 Hz, 1H; $C_{14}H_8N_2S_3$), 8.12 ppm (d, J = 4.0 Hz, 1H; $C_{14}H_8N_2S_3$); MS (FAB$^+$): m/z: 396.0 $[M]^+$.

[Pt(tctpy)(C≡C–C_4H_3S)][N*n*Bu$_4$]$_2$ (1): (2-Thiophen-5-ylethynyl)acetylene (22 mg, 0.21 mmol), a catalytic amount of CuI (1 mg), and NEt$_3$ (1 mL) were added to a degassed solution of [Pt(tctpy)]OTf (120 mg, 0.16 mmol) in DMF (10 mL). The resulting solution was stirred at room temperature for 5 h under an N_2 atmosphere. Upon addition of diethyl ether, a precipitate was formed, which was filtered, redissolved in DMF, and then filtered. Slow diffusion of diethyl ether vapor into this concentrated solution afforded the product as purple needle-shaped crystals. A metathesis reaction was carried out by adding 2 M tetrabutylammonium hydroxide (2.0 mL) to a hot aqueous solution of **1** with vigorous stirring. Chloroform (50 mL) was used to extract the product. Subsequent recrystallization of the complex was performed by the slow vapor diffusion of diethyl ether into a solution of the metathesized product in dichloromethane. Yield: 73 mg (36%); ^{1}H NMR (400 MHz, MeOD, 298 K, relative to Me$_4$Si): δ = 0.95 (t, J = 8.0 Hz, 24H; NBu$_4$), 1.4 (m, J = 8.0 Hz, 32H; NBu$_4$), 3.50 (t, J = 8.0 Hz, 16H; NBu$_4$), 7.00 (t, J = 4.0 Hz, 1H; C_3H_3S), 7.16 (d, J = 4.0 Hz; C_3H_3S), 7.26 (d, J = 4.0 Hz, 1H; C_3H_3S), 8.22 (d, J = 4.0 Hz, 2H; terpyridyl H), 8.82 (s, 2H; terpyridyl H), 8.87 (s, 2H; terpyridyl H), 9.18 ppm (d, J = 8.0 Hz, 2H; terpyridyl H); IR (KBr): $\tilde{\nu}$ = 2099 cm^{-1} (C≡C); MS (ESI): m/z: 667 $[M]^+$; elemental analysis calcd

(%) for $C_{56}H_{83}N_5O_6PtS{\cdot}CHCl_3$: C 53.98, H 6.67, N 5.51; found: C 54.37, H 6.78 N, 5.86.

[Pt(tctpy)(C≡C−$C_8H_5S_2$)][N*n*Bu$_4$]$_2$ (2): The procedure was similar to that for **1** except (2,2′-bithiophen-5-ylethynyl)acetylene (40 mg, 0.21 mmol) was used in place of (2-thiophen-5-ylethynyl)acetylene. Subsequent recrystallization of the complex was performed by the slow vapor diffusion of diethyl ether into a dichloromethane solution of the metathesized product. Yield: 67 mg (34%); ^{1}H NMR (400 MHz, MeOD, 298 K, relative to Me_4Si): $\delta = 0.95$ (t, $J = 8.0$ Hz, 24H; NBu_4), 1.4 (m, $J = 8.0$ Hz, 32H; NBu_4), 3.50 (t, $J = 8.0$ Hz, 16H; NBu_4), 6.74 (s, 1H; C_4H_3S), 6.85 (d, $J = 6.0$ Hz, 2H; C_4H_3S), 7.05 (s, 1H; C_4H_3S), 7.16 (d, $J = 6.0$ Hz, 1H; C_4H_3S), 8.04 (d, $J = 6.0$ Hz, 2H; terpyridyl H), 8.58 (s, 2H; terpyridyl H), 8.67 (s, 2H; terpyridyl H), 8.90 ppm (d, $J = 6.0$ Hz, 2H; terpyridyl H); IR (KBr): $\tilde{\nu} = 2099\ cm^{-1}$ (C≡C); MS (ESI$^+$): m/z: 749 $[M-OTf]^+$; elemental analysis calcd (%) for $C_{60}H_{85}N_5O_6PtS_2{\cdot}CH_2Cl_2$: C 55.66, H 6.41, N 5.32; found: C 55.89, H 6.12, N 5.28.

[Pt(tctpy)(C≡C−$C_8H_{10}N$)][N*n*Bu$_4$]$_2$ (3): The procedure was similar to that for complex **1** except 4-ethynyl-*N*,*N*-dimethylbenzenamine (30 mg, 0.21 mmol) was used in place of (2-thiophen-5-ylethynyl)acetylene. Subsequent recrystallization of the complex was performed by the slow vapor diffusion of diethyl ether into a solution of the metathesized product in dichloromethane. Yield: 57 mg (30%); ^{1}H NMR (400 MHz, MeOD, 298 K, relative to Me_4Si): $\delta = 0.95$ (t, $J = 8.0$ Hz, 24H; NBu_4), 1.4 (m, $J = 8.0$ Hz, 32H; NBu_4), 3.00 (s, 6H), 3.50 (t, $J = 8.0$ Hz, 16H; NBu_4), 6.72 (d, $J = 8.0$ Hz, 2H; C_6H_4), 7.46 (d, $J = 8.0$ Hz, 2H; C_6H_4), 8.22 (d, $J = 6.0$ Hz, 2H; terpyridyl H), 8.77 (s, 2H; terpyridyl H), 8.88 (s, 2H; terpyridyl H), 8.93 ppm (d, $J = 6.0$ Hz, 2H; terpyridyl H); IR (KBr): $\tilde{\nu} = 2099\ cm^{-1}$ (C≡C); MS (ESI$^+$): m/z: 702 $[M-OTf]^+$; elemental analysis calcd (%) for $C_{60}H_{90}N_6O_6Pt$: C 60.74, H 7.65, N 7.08; found: C 60.54, H 7.43, N 6.85.

[Pt(tctpy)(C≡C−$C_{14}H_7N_2S_3$)][N*n*Bu$_4$]$_2$ (4): The procedure was similar to that for **1**, except 4-(thiophen-2-yl)-7-{5-[(trimethylsilyl)ethynyl]thiophen-2-yl}benzo[*c*][1,2,5]thiadiazole (68 mg, 0.21 mmol) was used in place of 2-thiophen-5-ylethynylacetylene. Subsequent recrystallization of the complex was performed by the slow vapor diffusion of diethyl ether into a solution of the metathesized product in dichloromethane. Yield: 70 mg (32%); ^{1}H NMR (400 MHz, MeOD, 298 K, relative to Me_4Si): $\delta = 0.95$ (t, $J = 8.0$ Hz, 24H; NBu_4), 1.4 (m, $J = 8.0$ Hz, 32H; NBu_4), 3.00 (s, 6H) 3.50 (t, $J = 8.0$ Hz, 16H; NBu_4), 7.21 (t, $J = 4.0$ Hz, 1H; $C_{14}H_7N_2S_3$), 7.45 (d, $J = 4.0$ Hz, 2H; $C_{14}H_7N_2S_3$), 7.87 (d, $J = 4.0$ Hz, 2H; $C_{14}H_7N_2S_3$), 8.05 (d, $J = 4.0$ Hz, 1H; $C_{14}H_7N_2S_3$), 8.10 (s, $J = 4.0$ Hz, 1H; $C_{14}H_7N_2S_3$), 8.24 (d, $J = 6.0$ Hz, 2H; terpyridyl H), 8.78 (s, 2H; terpyridyl H), 8.88 (s, 2H; terpyridyl H), 9.18 ppm (d, $J = 6.0$ Hz, 2H; terpyridyl H); IR (KBr): $\tilde{\nu} = 2099\ cm^{-1}$ (C≡C); MS (ESI$^+$): m/z: 702 $[M-OTf]^+$; elemental analysis calcd (%) for $C_{66}H_{87}N_7O_6PtS_3$: C 58.04, H 6.42, N 7.18; found: C 58.18, H 6.58, N 7.43.

[Pt(dcbpy)(C≡C−C_4H_3S)$_2$] (5): 2-Ethynylthiophene (74 mg 0.69 mmol), a catalytic amount of CuI (1 mg), and NEt_3 (1 mL) were added to a degassed solution of [Pt(dctpy)] (160 mg, 0.31 mmol) in DMF (10 mL). The resulting solution was stirred at room temperature for 5 h under an N_2 atmosphere. Upon addition of diethyl ether, a precipitate was formed, which was filtered, redissolved in acetonitrile/methanol (3:2 v/v), and then filtered. Subsequent recrystallization of the complex was performed by the slow vapor diffusion of diethyl ether into acetonitrile/methanol to obtain a yellow solid. Yield: 131 mg (65%); ^{1}H NMR (300 MHz, CD_3SOCD_3, 298 K, relative to Me_4Si): $\delta = 6.97$ (d, $J = 6.0$ Hz, 2H; C_4H_3S), 7.06 (d, $J = 3.0$ Hz, 2H; C_4H_3S), 7.28 (d, $J = 6.0$ Hz, 2H; C_4H_3S), 8.17 (s, 2H; bipyridyl H), 8.84 (d, $J = 6.0$ Hz, 2H; bipyridyl H), 9.50 ppm (d, $J = 6.0$ Hz, 2H; bipyridyl H); IR (KBr): $\tilde{\nu} = 2110\ cm^{-1}$ (C≡C); MS (FAB$^+$): m/z: 654 $[M]^+$; elemental analysis calcd (%) for $C_{24}H_{14}N_2O_4PtS_2{\cdot}MeOH$: C 43.89, H 2.65, N 4.19; found: C 44.01, H 3.02, N 4.36.

[Pt(dcbpy)(C≡C−C_6H_5)$_2$] (6): The procedure was similar to that for complex **5**, except phenylacetylene (70 mg, 0.68 mmol) was used in place of 2-ethynylthiophene. The resulting solution was stirred at room temperature for 5 h under N_2 atmosphere. Upon addition of diethyl ether, a precipitate was formed, which was filtered, redissolved in acetonitrile/methanol (3:2 v/v), and then filtered. Subsequent recrystallization of the complex was performed by the slow vapor diffusion of diethyl ether into acetonitrile/methanol to obtain an orange solid. Yield: 110 mg (62%); ^{1}H NMR (300 MHz, CD_3SOCD_3, 298 K, relative to Me_4Si): $\delta = 7.18$ (t, $J = 6.0$ Hz, 4H; C_6H_5), 7.27 (t, $J = 6.0$ Hz, 4H; C_6H_5), 7.39 (d, $J = 6.0$ Hz, 4H; C_6H_5), 8.17 (s, 2H; bipyridyl H), 8.84 (d, $J = 6.0$ Hz, 2H; bipyridyl H), 9.50 ppm (d, $J = 6.0$ Hz, 2H; bipyridyl H); IR (KBr): $\tilde{\nu} = 2110\ cm^{-1}$ (C≡C); MS (FAB$^+$): m/z: 641 $[M]^+$; elemental analysis calcd (%) for $C_{28}H_{18}N_2O_4Pt{\cdot}MeOH{\cdot}MeCN$: C 52.10, H 3.83, N 5.88; found: C 52.06, H 4.03, N 5.97.

Physical measurements and instrumentation: ^{1}H NMR spectra were recorded using a Bruker AVANCE 400 (400 MHz) Fourier-transform NMR spectrometer with chemical shifts reported relative to tetramethylsilane ($(CH_3)_4Si$). Positive-ion fast atom bombardment (FAB) mass spectra were recorded using a Finnigan MAT95 mass spectrometer. IR spectra were obtained as Nujol mulls on KBr disks using a Bio-Rad FTS-7 Fourier transform infrared spectrophotometer (4000–400 cm^{-1}). Elemental analyses of the newly synthesized complexes were performed using a Flash EA 1112 elemental analyzer at the Institute of Chemistry, Chinese Academy of Sciences, Beijing.

The electronic absorption spectra were obtained using a Hewlett–Packard 8452A diode array spectrophotometer. The concentrations of solution samples for electronic absorption measurements were typically 7×10^{-5} mol dm^{-3}. Solid samples were freshly prepared and sonicated in a small sample vial that contained diethyl ether for an hour so that the sample was finely dispersed. The suspensions were directly used for solid-state electronic absorption and emission measurements. Steady-state excitation and emission spectra at room temperature and at 77 K were recorded using a Spex Fluorolog-3 Model FL3-211 fluorescence spectrofluorometer equipped with a R2658P PMT detector. Solid-state photophysical studies were carried out with solid samples contained in a quartz tube inside a quartz-walled Dewar flask. Measurements of the EtOH/MeOH (4:1 v/v) glass or solid-state sample at 77 K were similarly conducted with liquid nitrogen filled into the optical Dewar flask. The concentrations of the complex solutions in EtOH/MeOH (4:1 v/v) for glass-emission measurements were usually in the range of 10^{-6} mol dm^{-3}. All solutions for photophysical studies were degassed on a high-vacuum line in a two-compartment cell that consisted of a 10 mL Pyrex bulb and a 1 cm- or 4 mm-path-length quartz cuvette and sealed against the atmosphere by a Bibby Rotaflo HP6 Teflon stopper. The solutions were rigorously degassed with at least four successive freeze–pump–thaw cycles. Emission-lifetime measurements were performed using a conventional laser system. The excitation source used was a 355 nm output (third harmonic) of a Spectra-Physics Quanta-Ray Q-switched GCR-150-10 pulsed Nd:YAG laser. Luminescence decay signals were detected using a Hamamatsu R928 PMT instrument and recorded using a Tektronix Model TDS-620A (500 MHz, 2 GS s^{-1}) digital oscilloscope and analyzed using a program for exponential fits.

Cyclic voltammetric measurements were performed using a CH Instruments, Inc. model CHI 620A electrochemical analyzer. Electrochemical measurements were performed in *N*,*N*-dimethylformamide with 0.1 mol dm^{-3} nBu$_4$NPF$_6$ (TBAH) as supporting electrolyte at room temperature. The reference electrode was an Ag/$AgNO_3$ (0.1 mol dm^{-3} in acetonitrile) electrode, and the working electrode was a glassy carbon electrode (CH Instruments, Inc.) with a platinum wire as the counter electrode. The working electrode surface was first polished with 1 μm alumina slurry (Linde) on a microcloth (Buehler Co.) and then with 0.3 μm alumina slurry. It was then rinsed with ultra-pure deionized water and sonicated in a beaker that contained ultra-pure water for five minutes. The polishing and sonicating steps were repeated twice and then the working electrode was finally rinsed under a stream of ultra-pure deionized water. The ferrocenium/ferrocene couple ($FeCp_2^{+/0}$) was used as the internal reference.[31] All solutions for electrochemical studies were deaerated with prepurified argon gas prior to measurements.

Transient absorption measurements were performed using an LP920-KS Laser Flash Photolysis Spectrometer (Edinburgh Instruments Ltd, Livingston, UK) at ambient temperature. The excitation source was the 355 nm output (third harmonic) of an Nd:YAG laser (Quanta-Ray Lab-130 Pulsed Nd:YAG Laser) and the probe light source was a Xe900

450 W xenon arc lamp. The transient absorption spectra were detected using an image-intensified CCD camera (Andor) with PC plug-in controller, fully operated by L900 spectrometer software. The absorption kinetics were detected using a Hamamatsu R928 photomultiplier tube and recorded using a Tektronix Model TDS3012B (100 MHz, 1.25 GSs^{-1}) digital oscilloscope and analyzed using the same software for exponential fit (tail-fit data analysis). Samples were freshly prepared and degassed with at least four freeze–pump–thaw cycles on a high-vacuum line in a two-compartment cell that consisted of a 10 mL Pyrex bulb and a 1 cm-path-length quartz cuvette.

Dye-sensitized solar-cell (DSSC) fabrication: For DSSC fabrication, nanocrystalline-TiO_2-coated conducting glass substrates (ManSolar article 001) were used, whereas the counter electrodes were prepared by coating a drop of H_2PtCl_6 solution (2 mg Pt in 1 mL ethanol) with repetition of the heat treatment at 400 °C for 15 min. All measurements were performed in air without encapsulation and the measurements were made with a two-electrode arrangement that contained 0.6 M 1,3-dimethylimidazolium iodide (DMII), 0.05 M I_2, 0.5 M *tert*-butylpyridine (TBP), and 0.1 M LiI in methoxyacetonitrile. The TiO_2 electrodes were immersed in dye solutions for at least 16 h before use. Current–voltage characteristics of DSSC devices were measured using a programmable Keithley model 2400 power source. The photocurrent was measured under illumination from an Oriel 300W solar simulator equipped with an AM 1.5 G (AM: air mass; G: global) filter, and the light intensity was measured using an Oriel silicon reference cell. For the external quantum-efficiency measurements, devices were irradiated with monochromatic light of variable wavelength using an Oriel Cornerstone 260 1/4 m monochromator with a 300 W xenon arc lamp (Oriel Model no. 66984) as the light source. The intensity of the source at each wavelength was determined using a calibrated silicon detector (Oriel Model no. 71639). The photocurrent under short-circuit conditions was then recorded for each device at 10 nm intervals using a dual channel radiometer (Oriel Merlin Digital Lock-in Radiometry System Model no. 70104).

Computational details: Calculations were carried out using the Gaussian 03 software package.[21] Density functional theory (DFT) at the hybrid Perdew, Burke, and Ernzerhof functional (PBE0) level[22] was used to optimize the ground-state geometries of complexes **1** and **4**. Vibrational frequencies were calculated for all optimized geometries to verify that each was a minimum (NIMAG = 0) on the potential energy surface. The Stuttgart effective core potentials (ECPs) and the associated basis set was applied to describe for Pt[23] with an f polarization function (ζ_f(Pt) = 0.993),[24] whereas for all other atoms, the 6-31G(d,p) basis set[25a–c] was used. Based on the ground-state optimized geometries in the gas phase, the nonequilibrium time-dependent (TDDFT) method[26] at the same level associated with the conductorlike polarizable continuum model (CPCM)[27] was employed to compute the first twenty-five singlet–singlet transitions (CH_3OH as the solvent). For the TDDFT calculation, the same basis and effective core potentials as above were applied for Pt atoms, whereas for all the other atoms, a larger basis set of 6-31+G-(d,p)[25] was used.

Acknowledgements

V.W.-W.Y. acknowledges support from the University of Hong Kong under the Distinguished Research Achievement Award Scheme. E.C.-H.K. acknowledges the receipt of a postgraduate studentship from the University of Hong Kong. The work is supported by the University Grants Committee Areas of Excellence Scheme (AoE/P-03/08) and the Special Equipment Grant (SEG HKU07). We are grateful to Dr. Chi-Chiu Ko of the City University of Hong Kong for his assistance in photophysical measurements. We also thank the Computer Center at the University of Hong Kong for providing the computational resources.

[1] B. O'Regan, M. Grätzel, *Nature* **1991**, *353*, 737.
[2] M. K. Nazeeruddin, P. Péchy, T. Renouard, S. M. Zakeeruddin, R. Humphry-Baker, P. Comte, P. Liska, L. Cevey, E. Costa, V. Shklover, L. Spiccia, G. B. Deacon, C. A. Bignozzi, M. Grätzel, *J. Am. Chem. Soc.* **2001**, *123*, 1613.
[3] A. Juris, V. Balzani, F. Barigelletti, S. Campagna, P. Belser, A. von Zelewsky, *Coord. Chem. Rev.* **1988**, *84*, 85.
[4] K. Kalyanasundaram, *Coord. Chem. Rev.* **1982**, *46*, 159.
[5] K. Kalyanasundaram, M. Grätzel, *Coord. Chem. Rev.* **1998**, *177*, 347.
[6] M. T. Miller, P. K. Gantzel, T. B. Karpishin, *Inorg. Chem.* **1999**, *38*, 3414.
[7] Md. K. Nazeeruddin, C. Klein, P. Liska, M. Grätzel, *Coord. Chem. Rev.* **2005**, *249*, 1460.
[8] a) C. Klein, M. K. Nazeeruddin, P. Liska, D. D. Censo, N. Hirata, E. Palomares, J. R. Durrant, M. Grätzel, *Inorg. Chem.* **2005**, *44*, 178; b) C. Y. Chen, J. G. Chen, S. J. Wu, J. Y. Li, C. G. Wu, K. C. Ho, *Angew. Chem.* **2008**, *120*, 7452; *Angew. Chem. Int. Ed.* **2008**, *47*, 7342.
[9] a) M. K. Nazeeruddin, A. Kay, I. Rodicio, R. Humphry-Baker, E. Muller, P. Liska, N. Vlachopoulos, M. Grätzel, *J. Am. Chem. Soc.* **1993**, *115*, 6382; b) M. Yanagida, T. Yamaguchi, M. Kurashige, K. Hara, R. Katoh, H. Sugihara, H. Arakawa, *Inorg. Chem.* **2003**, *42*, 7921; c) R. Argazzi, C. A. Bignozzi, T. A. Heimer, F. N. Castellano, G. J. Meyer, *Inorg. Chem.* **1994**, *33*, 5741; d) T. A. Heimer, E. J. Heilweil, C. A. Bignozzi, G. J. Meyer, *J. Phys. Chem. A* **2000**, *104*, 4256.
[10] a) G. Sauvé, M. E. Cass, G. Coia, S. J. Doig, I. Lauermann, K. E. Pomykal, N. S. Lewis, *J. Phys. Chem. A* **2000**, *104*, 6821; b) G. M. Hasselmann, G. J. Z. Meyer, *Phys. Chem.* **1999**, *212*, 39.
[11] a) T. Bessho, E. C. Constable, M. Grätzel, A. Hernandez Redondo, C. E. Housecroft, W. Kylberg, M. K. Nazeeruddin, M. Neuburger, S. Schaffner, *Chem. Commun.* **2008**, 3717; b) M. T. Miller, P. K. Gantzel, T. B. Karpishin, *Inorg. Chem.* **1999**, *38*, 4314; c) Z. J. Ning, Q. Zhang, W. J. Wu, H. Tian, *J. Organomet. Chem.* **2009**, *694*, 2705; d) E. I. Mayo, K. Kilså, T. Tirrell, P. I. Djurovich, A. Tamayo, M. E. Thompson, N. S. Lewis, H. B. Gray, Photochem. Photobiol. Sci. **2006**, *5*, 871; e) J. R. Durrant, S. A. Haque, E. Palomores, *Coord. Chem. Rev.* **2004**, *248*, 1247; f) J. E. Moser, D. Noukakis, U. Bach, Y. Tachibana, D. R. Klug, J. R. Durrant, R. Humphry-Baker, M. Grätzel, *J. Phys. Chem. B* **1998**, *102*, 3649–3650; g) Y. Tachibana, J. E. Moser, M. Grätzel, D. R. Klug, J. R. Durrant, *J. Phys. Chem.* **1996**, *100*, 20056–20062.
[12] V. M. Miskowski, V. H. Houlding, *Inorg. Chem.* **1989**, *28*, 1529.
[13] a) A. Islam, H. Sugihara, K. Hara, L. P. Singh, R. Katoh, M. Yanagida, Y. Takahashi, S. Murata, H. Arakawa, *Inorg. Chem.* **2001**, *40*, 5371; b) J. Zhang, P. W. Du, J. Schneider, P. Jarosz, R. Eisenberg, *J. Am. Chem. Soc.* **2007**, *129*, 7726; c) S. Chakraborty, T. J. Wadas, H. Hester, R. Schmehl, R. Eisenberg, *Inorg. Chem.* **2005**, *44*, 6865; d) P. W. Du, K. Knowles R. Eisenberg, *J. Am. Chem. Soc.* **2008**, *130*, 12576; e) R. Okazaki, S. Masaoka, K. Sakai, *Dalton Trans.* **2009**, 6127; f) K. Yamauchi, S. Masaoka, K. Sakai, *J. Am. Chem. Soc.* **2009**, *131*, 8404; g) K. Sakai, H. Ozawa, *Coord. Chem. Rev.* **2007**, *251*, 2753; h) E. D. Cline, S. E. Adamson, S. Bernhard, *Inorg. Chem.* **2008**, *47*, 10378; i) L. L. Tinker, N. D. McDaniel, P. N. Curtin, C. K. Smith, M. J. Ireland, S. Bernhard, *Chem. Eur. J.* **2007**, *13*, 8726; j) J. I. Goldsmith, W. R. Hudson, M. S. Lowry, T. H. Anderson, S. Bernhard, *J. Am. Chem. Soc.* **2005**, *127*, 7502; k) US Patent, 6, 274, 806B1, **2001**; l) A. Hagfeldt, M. Grätzel, *Chem. Rev.* **1995**, *95*, 49.
[14] a) K. M. C. Wong, V. W. W. Yam, *Coord. Chem. Rev.* **2007**, *251*, 2477; b) K. M. C. Wong, W. S. Tang, B. W. K. Chu, N. Zhu, V. W. W. Yam, *Organometallics* **2004**, *23*, 3459; c) V. W. W. Yam, K. H. Y. Chan, K. M. C. Wong, N. Zhu, *Chem. Eur. J.* **2005**, *11*, 4535; d) K. M. C. Wong, W. S. Tang, X. X. Lu, N. Y. Zhu, V. W. W. Yam, *Inorg. Chem.* **2005**, *44*, 1492; e) V. W. W. Yam, R. P. L. Tang, K. M. C. Wong, K. K. Cheung, *Organometallics* **2001**, *20*, 4476; f) J. A. Bailey, M. G. Hill, R. E. Marsh, V. M. Miskowski, W. P. Schaefer, H. B. Gray, *Inorg. Chem.* **1995**, *34*, 4591; g) G. T. Morgan, F. H. Burstall, *J. Chem. Soc.* **1934**, 1498; h) M. Howe-Grant, S. Lippard, *Inorg. Synth.* **1980**, *20*, 101; i) I. E. Pomestchenko, C. R. Luman, M. Hissler, R. Ziessel, F. N. Castellano, *Inorg. Chem.* **2003**, *42*, 1394.

[15] a) S. Chakraborty, T. J. Wadas, H. Hester, C. Flaschenreim, R. Schmehl, R. Eisenberg, *Inorg. Chem.* **2005**, *44*, 6284; b) W. B. Connick, D. Geiger, R. Eisenberg, *Inorg. Chem.* **1999**, *38*, 3264; c) W. B. Connick, D. Geiger, R. Eisenberg, *Inorg. Chem.* **1999**, *38*, 3264.

[16] a) C. W. Chan, L. K. Cheng, C. M. Che, Y. Wang, *Coord. Chem. Rev.* **1994**, *132*, 87; b) S. C. Chan, M. C. W. Chan, Y. Wang, C. M. Che, K. K. Cheung, N. Y. Zhu, *Chem. Eur. J.* **2001**, *7*, 4180; c) C. E. Whittle, J. A. Weinstein, M. W. George, K. S. Schanze, *Inorg. Chem.* **2001**, *40*, 4053; d) F. Hua, S. Kinayyigit, J. R. Cable, F. N. Castellano, *Inorg. Chem.* **2005**, *44*, 471.

[17] a) Q. Z. Yang, L. Z. Wu, Z. W. Wu, L. P. Zhang, C. H. Tung, *Inorg. Chem.* **2002**, *41*, 5653; b) X. Han, L. Z. Wu, G. Si, J. Pan, Q. Z. Yang, L. P. Zhang, C. H. Tung, *Chem. Eur. J.* **2007**, *13*, 1231.

[18] T. W. Hamann, R. A. Jensen, A. B. F. Martinson, H. V. Ryswyk, J. T. Hupp, *Energy Environ. Sci.* **2008**, *1*, 66.

[19] a) D. Zhang, L.-Z. Wu, L. Zhou, X. Han, Q.-Z. Yang, L.-P. Zhang, C.-H. Tung, *J. Am. Chem. Soc.* **2004**, *126*, 3440; b) P. Jarosz, J. Thall, J. Schneider, D. Kumaresan, R. Schmehl, R. Eisenberg, *Energy Environ. Sci.* **2008**, *1*, 573; c) E. Shikhova, E. O. Danilov, S. Kinayyigit, I. E. Pomestchenko, A. D. Tregubov, F. Camerel, P. Retailleau, R. Ziessel, F. N. Castellano, *Inorg. Chem.* **2007**, *46*, 3038; d) E. O. Danilov, I. E. Pomestchenko, S. Kinayyigit, P. L. Gentili, M. Hissler, R. Ziessel, F. N. Castellano, *J. Phys. Chem. A* **2005**, *109*, 2465; e) F. N. Castellano, I. E. Pomestchenko, E. Shikhova, F. Hua, M. L. Muro, N. Rajapakse, *Coord. Chem. Rev.* **2006**, *250*, 1819; f) P. Jarosz, P. Du, J. Schneider, S. H. Lee, D. McCamant, R. Eisenberg, *Inorg. Chem.* **2009**, *48*, 9653; g) P. Jarosz, K. Lotito, J. Schneider, D. Kumaresan, R. Schmehl, R. Eisenberg, *Inorg. Chem.* **2009**, *48*, 2420.

[20] a) J. G. Mei, K. Ogawa, Y.-G. Kim, N. C. Heston, D. J. Arenas, Z. Nasrollahi, T. D. McCarley, D. B. Tanner, J. R. Reynolds, K. S. Schanze, *ACS Appl. Mater. Interfaces* **2009**, *1*, 150; b) F. Guo, Y. G. Kim, J. R. Reynolds, K. S. Schanze, *Chem. Commun.* **2006**, *17*, 1887; c) F. Guo, K. Ogawa, Y. G. Kim, E. O. Danilov, F. N. Castellano, J. R. Reynoldsa, K. S. Schanze, *Phys. Chem. Chem. Phys.* **2007**, *9*, 2601; d) D. Kumaresan, K. Lebkowsky, R. H. Schmehl, *J. Photochem. Photobiol. A* 2009, 207, 86; e) S. Suzuki, R. Sugimura, M. Kozaki, K. Keyaki, K. Nozaki, N. Ikeda, K. Akiyama, K. Okada, *J. Am. Chem. Soc.* **2009**, *131*, 10374.

[21] Gaussian 03, Revision E.01, M. J. Frisch, G. W. Trucks, H. B. Schlegel, G. E. Scuseria, M. A. Robb, J. R. Cheeseman, J. A. Montgomery, Jr., T. Vreven, K. N. Kudin, J. C. Burant, J. M. Millam, S. S. Iyengar, J. Tomasi, V. Barone, B. Mennucci, M. Cossi, G. Scalmani, N. Rega, G. A. Petersson, H. Nakatsuji, M. Hada, M. Ehara, K. Toyota, R. Fukuda, J. Hasegawa, M. Ishida, T. Nakajima, Y. Honda, O. Kitao, H. Nakai, M. Klene, X. Li, J. E. Knox, H. P. Hratchian, J. B. Cross, V. Bakken, C. Adamo, J. Jaramillo, R. Gomperts, R. E. Stratmann, O. Yazyev, A. J. Austin, R. Cammi, C. Pomelli, J. W. Ochterski, P. Y. Ayala, K. Morokuma, G. A. Voth, P. Salvador, J. J. Dannenberg, V. G. Zakrzewski, S. Dapprich, A. D. Daniels, M. C. Strain, O. Farkas, D. K. Malick, A. D. Rabuck, K. Raghavachari, J. B. Foresman, J. V. Ortiz, Q. Cui, A. G. Baboul, S. Clifford, J. Cioslowski, B. B. Stefanov, G. Liu, A. Liashenko, P. Piskorz, I. Komaromi, R. L. Martin, D. J. Fox, T. Keith, M. A. Al-Laham, C. Y. Peng, A. Nanayakkara, M. Challacombe, P. M. W. Gill, B. Johnson, W. Chen, M. W. Wong, C. Gonzalez, J. A. Pople, Gaussian, Inc., Wallingford CT, **2004**.

[22] a) M. Ernzerhof, G. E. Scuseria, *J. Chem. Phys.* **1999**, *110*, 5029; b) M. Ernzerhof, J. P. Perdew, K. Burke, *Int. J. Quantum Chem.* **1997**, *64*, 285.

[23] D. Andrae, U. Häussermann, M. Dolg, H. Stoll, H. Preuss, *Theor. Chim. Acta* **1990**, **77**, 123.

[24] A. W. Ehlers, M. Böhme, S. Dapprich, A. Gobbi, A. Höllwarth, V. Jonas, K. F. Köhler, R. Stegmann, A. Veldkamp, G. Frenking, *Chem. Phys. Lett.* **1993**, *208*, 111.

[25] a) W. J. Hehre, R. Ditchfield, J. A. Pople, *J. Chem. Phys.* **1972**, *56*, 2257; b) P. C. Hariharan, J. A. Pople, *Theor. Chim. Acta* **1973**, *28*, 213; c) M. M. Francl, W. J. Pietro, W. J. Hehre, J. S. Binkley, M. S. Gordon, D. J. Defrees, J. A. Pople, *J. Chem. Phys.* **1982**, *77*, 3654; d) T. Clark, J. Chandrasekhar, G. W. Spitznagel, P. von R. Schleyer, *J. Comput. Chem.* **1983**, *4*, 294; e) G. W. Spitznagel, T. Clark, P. von R. Schleyer, W. J. Hehre, *J. Comput. Chem.* **1987**, *8*, 1109.

[26] a) R. E. Stratmann, G. E. Scuseria, M. J. Frisch, *J. Chem. Phys.* **1998**, *109*, 8218; b) R. Bauernschmitt, R. Ahlrichs, *Chem. Phys. Lett.* **1996**, *256*, 454; c) M. E. Casida, C. Jamorski, K. C. Casida, D. R. Salahub, *J. Chem. Phys.* **1998**, *108*, 4439.

[27] a) V. Barone, M. J. Cossi, *J. Phys. Chem. A* **1998**, *102*, 1995; b) M. Cossi, N. Rega, G. Scalmani, V. Barone, *J. Comput. Chem.* **2003**, *24*, 669.

[28] H. Shu, K. Toshifumi, *J. Heterocycl. Chem.* **2003**, *40*, 845.

[29] J. L. Wang, Z. Ming; X. Qi, Ma, Yuguo, J. Pei, *Org. Lett.* **2009**, *11*, 863; X. Qi, Ma, Yuguo, J. Pei, *Org. Lett.* **2009**, *11*, 863.

[30] R. R. Gagne, C. A. Koval, G. C. Lisensky, *Inorg. Chem.* **1980**, *19*, 2854.

[31] R. R. Gagne, C. A. Koval, G. C. Lisensky, *Inorg. Chem.* **1980**, *19*, 2854.

Received: May 22, 2010
Published online: September 14, 2010

